Momentum-space entanglement after a quench in one-dimensional disordered fermionic systems

Rex Lundgren,[1] Fangli Liu,[1] Pontus Laurell,[2] and Gregory A. Fiete[3,4]

[1]*Joint Quantum Institute, NIST/University of Maryland, College Park, MD 20742, USA*
[2]*Center for Nanophase Materials Sciences, Oak Ridge National Laboratory, Oak Ridge, TN 37831, USA*
[3]*Department of Physics, Northeastern University, Boston, MA 02115, USA*
[4]*Department of Physics, Massachusetts Institute of Technology, Cambridge, MA 02139, USA*

We numerically investigate the momentum-space entanglement entropy and entanglement spectrum of the random-dimer model and its generalizations, which circumvent Anderson localization, after a quench in the Hamiltonian parameters. The type of dynamics that occurs depends on whether or not the Fermi level of the initial state is near the energy of the delocalized states present in these models. If the Fermi level of the initial state is near the energy of the delocalized states, we observe an interesting slow logarithmic-like growth of the momentum-space entanglement entropy followed by an eventual saturation. Otherwise, the momentum-space entanglement entropy is found to rapidly saturate. We also find that the momentum-space entanglement spectrum reveals the presence of delocalized states in these models for long times after the quench and the many-body entanglement gap decays logarithmically in time when the Fermi level is near the energy of the delocalized states.

Introduction.—The growth of entanglement after a sudden quantum quench in many-body systems has been an active research area over the past decade and has even been experimentally observed [1]. Typically, the entanglement entropy (EE) and entanglement spectrum (ES) [2] are used to quantify entanglement. To calculate the ES, one forms the density matrix, $\rho(t)$, from a pure quantum state, $|\psi(t)\rangle$. The Hilbert space is then partitioned into two regions, A and B. Region B is traced over, giving the reduced density matrix, $\rho_A(t) = \mathrm{Tr}_B(\rho(t))$. The ES is related to the eigenvalues of ρ_A. From it, one obtains the more commonly studied EE, $S(t) = -\mathrm{Tr}[\rho_A(t)\ln(\rho_A(t))]$. Real-space EE in one-dimension (1D) after a quench has well-known behaviour. For example, for a generic 1D system with translational invariance, the EE typically grows linearly until it saturates with a volume dependence [3–6]. Such behavior can be understood from a quasi-particle picture [3] or operator spreading [6]. For Anderson-localized 1D systems the EE initially grows ballistically and then saturates to an area law [7, 8]. In many-body localized systems, $S(t)$ grows logarithmically (after some initial power-law like growth) [7, 9, 10]. While there have been several works on the real-space ES after a quench [11–22], no general results have emerged.

On the other hand, the (ground-state) EE and ES between novel bipartitions of the many-body Hilbert-space have proven useful for investigating exotic phases of matter. Notable examples include the EE and ES between left-and right-movers in 1D [23–29] and the bulk ES [30–33]. The latter can reveal topological order and probe topological phase transitions from a single wavefunction [30] and the former has highlighted an interesting connection between fractional quantum Hall systems and critical quantum spin chains [23]. Entanglement between left-and right-moving particles, i.e. momentum-space entanglement, is useful in identifying delocalized states and the delocalization-localization transition in 1D disordered systems [34–38]. With just a single disorder configuration, the momentum-space ES can reveal the presence of delocalized states in several 1D disordered models with correlated disorder. These models include the random-dimer model (and its generalizations) [34, 35], the Aubry-André model [35] and a model with long-range correlated disorder [36]. The momentum-space ES can also reveal the critical point in interacting disordered models [38]. We note momentum-space entanglement has also been studied in high-energy physics [39–44].

More recently, momentum-space entanglement in Tomonaga-Luttinger liquids was studied after a quench of Hamiltonian parameters (quantum quench) [45]. It was found that the momentum-space EE saturates quickly, drastically different from the rapid entanglement growth in real-space typically observed, and that the entanglement gap (difference between the two lowest levels of the ES) is a universal function of the Luttinger parameter. Furthermore, it was shown that ES levels are given by the overlap of certain states with the initial state, allowing for the momentum-space EE and ES to be measured experimentally for Tomonaga-Luttinger liquids.

In this work, we numerically investigate the momentum-space EE and ES of the non-interacting random-dimer model and its generalizations after a global quantum quench from a clean to disordered system. If the Fermi level of the initial state is near the energy of the delocalized states of these models (and the disorder strength is far below its critical value), the momentum-space EE grows logarithmically-like until it eventually saturates. When the Fermi level of the initial state is far away from the energy of the delocalized states, the momentum-space EE rapidly saturates. We argue that this behavior is due to the absence of backscattering between degenerate states near the energies of the delocalized states of these models. We also find the ES reveals the presence of delocalized states for long times after the quench and the many-body entanglement gap decays logarithmically in time when the Fermi level is near resonance. To the best of our knowledge, such slow growth of entanglement has only been seen in real-space EE and our work provides the first example of slow entanglement growth for a non-local Hilbert space bipartition. Furthermore, the fact that the momentum-space EE saturates (either slowly or rapidly) and the entanglement gap remains open might prove useful for momentum-space based density renormalization group algorithms [46, 47].

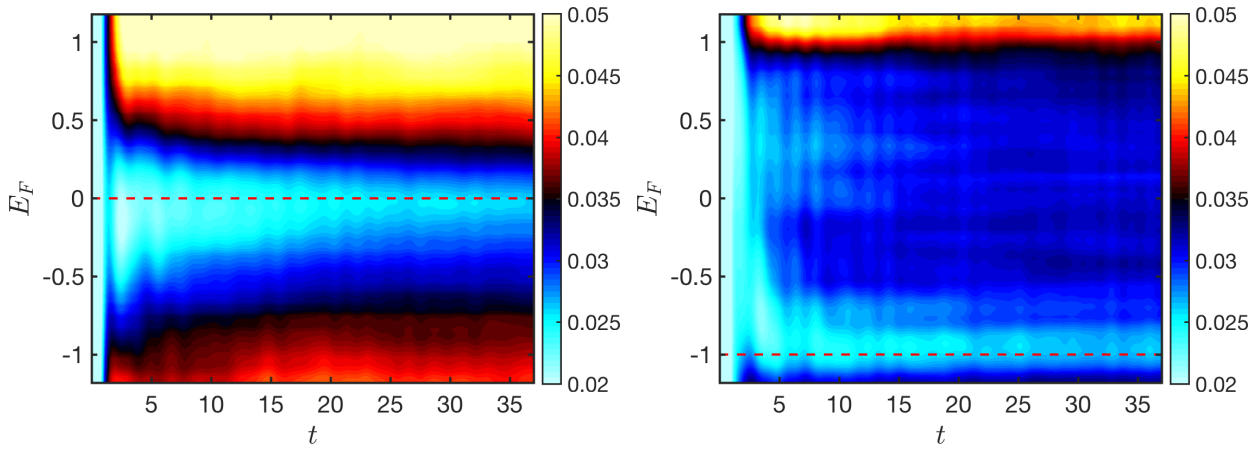

(a) Random-dimer Model (b) Random-trimer Model

FIG. 1. (color online) EE between left-and right-movers (divided by N) for a single disorder configuration of the random-dimer model (a) and the random-trimer model (b) as a function of t and doping level of initial state. There is a clear suppression of entanglement for initial states with E_F near the resonant energies of these models (dashed red lines). Parameters: $N = 702$ and $\epsilon_b = -3/4$.

Random-dimer model.—We now review the random-dimer model, originally introduced by P. Phillips *et al.* [48], and its generalizations [49]. The Hamiltonian of this model (and its generalizations) is of the form,

$$H = J\sum_{i=1}^{N}\left(c_{i+1}^{\dagger}c_i + c_i^{\dagger}c_{i+1}\right) + \sum_{i=1}^{N}\epsilon_i c_i^{\dagger}c_i, \qquad (1)$$

where $c_i^{\dagger}$ is the creation operator for an electron on site i, ϵ_i is the on-site energy, N is the system size, and J is the hopping energy, which is set to one without loss of generality. Throughout this work, we take $N = 4n + 2$, where $n \in \mathbb{Z}$, to avoid a degenerate Fermi sea. For the random-dimer model, ϵ_i is restricted to two discrete values, ϵ_a and ϵ_b, and one of the on-site energies always appears in pairs, i.e. on two consecutive sites. Without loss of generality, ϵ_a is taken to be zero and always appears in pairs and ϵ_a and ϵ_b have an equal probability of appearing. In this case, a delocalized state exists at $E = 0$ for $|\epsilon_b| < 2J$. We will refer to single-particle energies at which delocalized states exist as resonances. There are generalizations of this model, where instead of ϵ_a always appearing in pairs, it appears in groups of three or more [49]. In addition to the random-dimer model, we consider the case when ϵ_b always appears in groups of three, which is called the random-trimer model. For the random-trimer model, there exist delocalized states at $E = \pm J$. The delocalized state at $E = J(-J)$ persists for $-J < \epsilon_b < 3J(-3J < \epsilon_b < J)$. We note that real-space entanglement properties of these models have been investigated in Refs. [34, 35, 37, 50, 51].

Fourier transforming the electronic creation operator, $c_x^{\dagger} = \frac{1}{\sqrt{N}}\sum_{k=0}^{N-1} e^{i2\pi kx/N}c_k^{\dagger}$, yields,

$$H = \sum_{k,k'=0}^{N-1}\left(2J\cos(\frac{2\pi}{N}k)\delta_{k,k'} + V_{k,k'}\right)c_k^{\dagger}c_{k'} \quad , \qquad (2)$$

where $V_{k,k'} = \sum_{x=1}^{N}\epsilon_x e^{i\frac{2\pi}{N}x(k-k')}$ is the scattering matrix in momentum-space. We see that disorder induces entanglement between different momentum modes, making a momentum-space partition particularly natural.

Formalism.—To calculate entanglement, we use the formalism introduced in Ref. [52] which allows one to calculate entanglement for large non-interacting systems. More specifically, to compute entanglement properties, we only need the two-point correlation function, $\langle\psi(t)|c_k^{\dagger}c_{k'}|\psi(t)\rangle$. To begin, we first diagonalize our Hamiltonian via a unitary transformation, U. This gives $H = \sum_{r=0}^{N-1}\epsilon_r d_r^{\dagger}d_r$, where ϵ_r are the single-particle energy levels of the disordered system and $c_k = \sum_{r=0}^{N-1}U_{kr}d_r$. We take our initial state, $|\psi_0\rangle$, to be the ground state of the clean system ($\epsilon_i = 0\ \forall\ i$) with a variable Fermi level, i.e. $|\psi_0\rangle = \prod_{k=k_i}^{k_f}c_k^{\dagger}|0\rangle$. For example, at half-filling, $k_i = N/4 + 1/2$ and $k_f = 3N/4 - 1/2$. We label the Fermi level of the initial state, E_F, by the single-particle energy to which the post-quench Hamiltonian is filled. We always vary the number of total particles by two to avoid a degenerate Fermi sea. The wavefunction of the system evolves as $|\psi(t)\rangle = e^{-iHt}|\psi_0\rangle$, where t is the time after the quench. We restrict ourselves to weak quenches, i.e. disorder strengths much less than the disorder strength at which all states become delocalized. The correlation function, which depends on E_F, is given by

$$\langle\psi(t)|c_k^{\dagger}c_{k'}|\psi(t)\rangle = \sum_{s,r=0}^{N-1}T_{s,r}U_{ks}^{*}U_{k'r}e^{-i(E_r-E_s)t}, \qquad (3)$$

where $T_{s,r} = \sum_{k''=k_i}^{k_f}(U_{sk''}^{-1})^{*}U_{rk''}^{-1}$. $\langle\psi(t)|c_k^{\dagger}c_{k'}|\psi(t)\rangle$ is calculated numerically for all left-moving momenta $(k, k' \in \{0, 1, \ldots, N/2 - 1\})$ [45]. The ES and EE between left-and right-movers can be obtained from the eigenvalues of this $N/2$ by $N/2$ correlation matrix. More specifically, the reduced density matrix is given by $\rho_A(t) =$

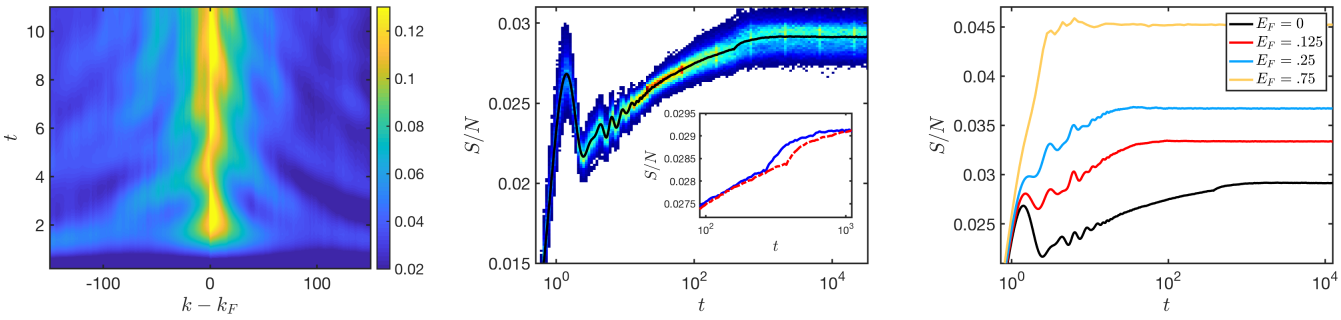

(a) (b) (c)

FIG. 2. (color online) (a) $C_s(k)$ as a function of t and momentum for $E_F \approx 0$ (for a single disorder configuration). Momentum modes near the Fermi momentum of $|\psi_0\rangle$ give rise to the largest contribution to $S(t)$. (b) Distribution of $S(t)/N$ of the random-dimer model as a function of t for various disorder configurations. Solid black line is disorder averaged $S(t)/N$. A clear slow logarithmic-like growth is observed for intermediate times. Inset: $S(t)/N$ for $N = 502$ (solid-blue line) and $N = 702$ (dashed-red line). For early enough times, the curves lie on top of each other demonstrating that $S(t)$ obeys a volume law. (c) Disorder averaged $S(t)/N$ of the random-dimer model versus t for various E_F . For large enough E_F, there is no apparent logarithmic-like growth and $S(t)$ saturates. Parameters: $N = 702$ and $\epsilon_b = -3/4$.

$\exp\left[\sum_{g=0}^{N/2-1} \epsilon_g(t)\chi_g^\dagger\chi_g\right]$, where $\epsilon_g(t)$ is the single-particle ES and $\chi_g^\dagger$ is a linear combination of $c_k^\dagger$. The single-particle ES is related to the eigenvalues of the correlation matrix, $\xi_g(t)$, as follows $\xi_g(t) = (e^{\epsilon_g(t)} + 1)^{-1}$. The EE is then, $S(t) = \sum_{g=0}^{N/2-1} S_g(t)$, where $S_g(t) = -(\xi_g \ln(\xi_g) + (1 - \xi_g)\ln(1 - \xi_g))$. As seen from $S_g(t)$, correlation eigenvalues near 1/2 contribute the most.

Momentum-space entanglement entropy.—We now are in a position to calculate the momentum-space EE. We first note that the momentum-space EE is numerically found to scale linearly with N for all parameters and times, i.e. $S(t)$ obeys a volume law (up to some finite-size effects, which are discussed later). This can be seen by disorder averaging for two different N while keeping E_F and ϵ_B fixed [53]. The momentum-space EE of Tomonaga-Luttinger liquids after a quench was also found to obey a volume law for all times [45].

In Fig. 1a, $S(t)$ is plotted as a function of time and E_F for the random-dimer model for a single disorder configuration. Momentum-space EE growth is clearly suppressed for initial states with $E_F \approx 0$, which is the energy of the delocalized state of the random-dimer model. Note, this does not correspond to a half-filled initial state. In Fig. 1b, we plot the momentum-space EE for the random-trimer model. Again, there is a suppression of EE growth near a delocalized state of the random-trimer model, $E_F = -1$ (the other delocalized state at $E_F = 1$ is close to becoming localized for $\epsilon_b = -3/4$, so the suppression does not appear).

We now turn to gaining a qualitative understanding of this observation. In general, this is a challenging problem as a single-particle eigenstate of the clean system has overlap with all single-particle disordered eigenstates [54]. However, weak disorder (in our case, $\epsilon_B \ll 4J$) only mixes momentum states that are close in energy. Therefore, which momentum-modes contribute to momentum-space entanglement? To quantify this, we look at the entanglement contour [55], which is given by $C_s(k) = \sum_{g=0}^{N/2-1} |\phi_k(g)|^2 S_g$, where $\phi_k(g)$ describes the momentum structure of the gth eigenvector of the correlation matrix. Summing $C_s(k)$ over all k in region A yields $S(t)$. This quantity has been used to investigate which real-space modes contribute to the entanglement between spatial regions. As expected, for real-space entanglement, modes near the bipartition give rise to a larger contribution. In our case, we numerically find (after some transient behavior in which a wide range of momentum modes contribute) only momentum modes near the Fermi surface contribute to entanglement for weak quenches, regardless of E_F (see Fig. 2a). We are now in a position to qualitatively understand the features seen in Fig. 1. For the random-dimer model (and its generalizations), backscattering between degenerate single-particle states with the same energy as the delocalized state is suppressed [10]. Given these two facts, we expect $S(t)$ to be suppressed when E_F is near resonance. Indeed, we observe this numerically (see Fig. 1).

We now investigate how fast momentum-space entanglement grows. In Fig. 2b, we plot the distribution of momentum-space EE (for the random-dimer model) versus time for five-hundred disorder configurations, along with the disorder averaged EE, when $E_F \approx 0$. After initial power-law like growth, a slow logarithmic-like growth is observed at intermediate times. Finally, at late times, there is eventual saturation. This slow growth occurs for all disordered configurations considered. We note the kink around $t \approx 400$ in Fig. 2b is a finite-size effect and is found to appear at later times as one increases N (see inset of Fig. 2b). We believe the presence of this finite-size effect is indicative of the delocalized state present at $E_F = 0$. Upon varying E_F, the saturation time decreases, the saturation value increases, and the rate at which the EE grows increases (slope of log growth). This is illustrated in Fig. 2c. For large enough E_F, our system size is greater than the localization length. Thus, there are no finite-size effects and no sharp kinks, in contrast to when E_F is at resonance. Finally, when

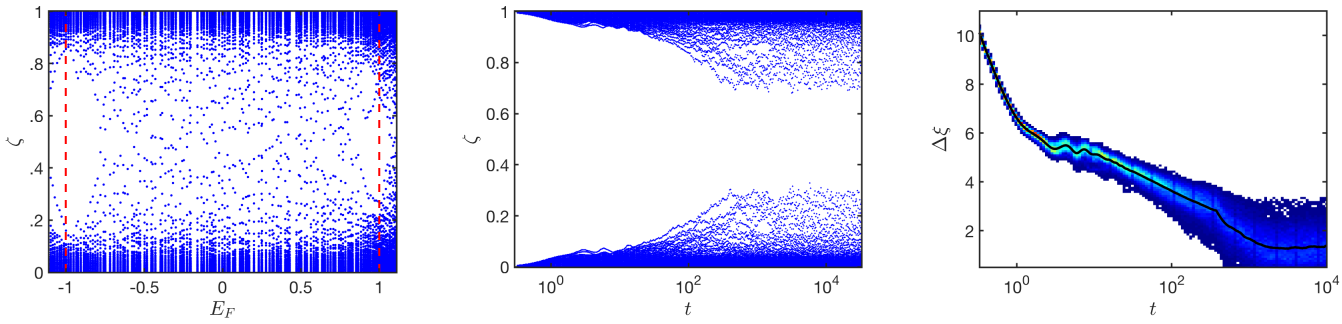

FIG. 3. (color online) (a) Single-particle ES of the random-trimer model as a function of E_F for $t = 50$. When E_F is near resonance (dashed red lines), there is a gap in the single-particle ES for long-times (b) Single-particle ES of the random-dimer model as a function of t for $E_F = 0$. The single-particle entanglement gap remains for long-times. (c) Distribution of $\Delta\xi$ versus t for the random-dimer model (at resonance) for various disorder configurations. The solid-black line is the disorder averaged entanglement gap. $\Delta\xi$ decays logarithmically after some initial power-law like decay. The kink observed at $t \approx 400$ is a finite-size effect and occurs at later times as N increases. Here, $N_A = 189$. Parameters: $N = 702$ and $\epsilon_b = -3/4$.

E_F is far enough away from resonance, there is no longer any logarithmic-like growth of EE and it rapidly saturates, as shown in Fig. 2c. We conjecture this slow growth is due to the absence of single-particle backscattering between degenerate states near resonance. As such, any entanglement between momentum modes would be induced by scattering between non-degenerate states, which is a suppressed process for weak disorder [54]. Hence, momentum-space EE grows slowly. It would be desirable to prove this conjecture analytically. We leave this as an open problem.

We now ask if this logarithmic-like growth is related to logarithmic growth observed in the real-space EE dynamics of various models. These models include 1D many-body localized systems [7, 9, 10] (including quasi-many-body localization [56]), 1D non-interacting fermions with integrable disorder [57], the central-spin model [58], a two-dimensional non-interacting disordered fermion system with potential disorder [59], and, perhaps counter-intuitively, 1D translationally-invariant spin chains with long-range interactions [60, 61] and 1D disordered fermions with long-range hopping [62, 63]. For the 1D systems mentioned above, the EE grows as $S(t) \propto \log(t)$, while in our case, it grows as $S(t) \propto N\log(t)$, i.e. a volume law for all times, strongly indicating a different mechanism is responsible for the dynamics we observe [64]. For the two-dimensional disordered system, the real-space EE grows as $S(t) \propto N\log(t)$ [59]. However, the authors of Ref. [59] relate this slow growth to logarithmic connections that arise in two-dimensions. Given that our model is one-dimensional, their argument likely cannot explain our results. We therefore conclude the logarithmic growth we observe *is not related* to the logarithmic growth that has been previously observed in real-space for various models.

Entanglement spectra.—We now turn to the ES, which may reveal more information [2]. We first consider the single-particle ES (eigenvalues of the correlation matrix) after a quench and investigate the single-particle ES as a function of E_F of the initial state for a fixed time. We find that when E_F is near resonance, there is a gap in the single-particle ES (see Fig. 3a), signaling the presence of delocalized states. This behavior is reminiscent of the single-particle ES of the ground-state wavefunction [34], where the single-particle ES also reveals the presence of delocalized states. Furthermore, the resonance at $E_F = 1$ is more apparent compared to the EE (see Fig. 1b), signaling a possible advantage of the ES over the EE in revealing this phyiscs. The single-particle entanglement gap (at resonance) remains open for long-times after a quench, as shown in Fig. 3b for the random-dimer model.

One can also consider the many-body ES. We investigate the difference between the two lowest eigenvalues of the many-body ES, which is referred to as the many-body entanglement gap [65], $\Delta\xi$. Upon fixing the number of particles in region A, N_A, the gap $\Delta\xi$ can be expressed in terms of the single-particle ES as follows, $\Delta\xi = \epsilon_{g=N/4+x-1/2}(t) - \epsilon_{g=N/4+x+1/2}(t)$, where x is the number of left-moving particles above or below half-filling (for half-filling, $x = 0$). In general, one can construct the exact many-body ES from $\epsilon_g(t)$, but this is time consuming (as well as limited by computational resources) because one must take products of single-particle ES. At resonance, $\Delta\xi$ is found to decrease logarithmically after some initial-power law like decay (see Fig. 3c). In contrast, for clean interacting systems, $\Delta\xi$ was found to saturate rapidly after a quench [45]. This slow logarithmic decay continues until $t \approx 400$, at which time finite-size effects become important (this is the same time at which finite-size effects occur for $S(t)$, as seen in Fig. 2b). Due to this finite-size effect, we can not investigate whether or not $\Delta\xi$ closes. Finally, we note that doping away from resonance (or increasing ϵ_b) increases the rate at which $\Delta\xi$ decreases.

Discussion.— We have investigated the entanglement between left- and right-movers after a quench for the random-dimer model and its generalizations. We found that there is a suppression of momentum-space entanglement and that momentum-space entanglement entropy features logarithmic-like growth when the Fermi level of the initial state is at a

certain energy (the energy of the delocalized states present in these models). We also found that the momentum-space entanglement spectrum has clear signatures of the delocalized states present in these models and the entanglement gap decays logarithmically. In the future it would be interesting to develop an analytical theory for the above results and investigate the effect of interactions on entanglement dynamics for the random-dimer model [66]. The latter problem is particularly interesting as the interacting random-dimer model circumvents the Imry-Ma argument [67]. It would also be worthwhile to see if our results (the saturation of entanglement entropy and presence of an entanglement gap) could be used to develop efficient momentum-space density matrix renormalization group algorithms.

ACKNOWLEDGMENTS

We are grateful to T. Hughes, I. Mondragon-Shem, A. V. Gorshkov, F. Pollmann, V. Chua, P. Titum, J. Garrison, Z. Yang, X. Li, and H. Changlani for useful discussions. R.L. and F.L. acknowledge support by the DoE BES QIS program (award No. DE-SC0019449), AFOSR, DoE ASCR Quantum Testbed Pathfinder program (award No. DE-SC0019040), NSF PFCQC program, NSF PFC at JQI, ARO MURI, and ARL CDQI. P.L. acknowledges support from the Scientific Discovery through Advanced Computing (SciDAC) program funded by the US Department of Energy, Office of Science, Advanced Scientific Computing Research and Basic Energy Sciences, Division of Materials Sciences and Engineering. G.A.F. is grateful for funding under NSF DMREF Grant no DMR-1949701 and NSF Materials Research Science and Engineering Center Grant No. DMR-1720595. The authors acknowledge the University of Maryland supercomputing resources made available for conducting the research reported in this work.

[1] Rajibul Islam, Ruichao Ma, Philipp M Preiss, M Eric Tai, Alexander Lukin, Matthew Rispoli, and Markus Greiner, "Measuring entanglement entropy in a quantum many-body system," Nature **528**, 77 (2015).

[2] Hui Li and F. D. M. Haldane, "Entanglement spectrum as a generalization of entanglement entropy: Identification of topological order in non-abelian fractional quantum hall effect states," Phys. Rev. Lett. **101**, 010504 (2008).

[3] P. Calabrese and J. Cardy, "Evolution of entanglement entropy in one-dimensional systems," Journal of Statistical Mechanics: Theory and Experiment **4**, 04010 (2005), cond-mat/0503393.

[4] Gabriele De Chiara, Simone Montangero, Pasquale Calabrese, and Rosario Fazio, "Entanglement entropy dynamics of heisenberg chains," Journal of Statistical Mechanics: Theory and Experiment **2006**, P03001 (2006).

[5] Hyungwon Kim and David A. Huse, "Ballistic spreading of entanglement in a diffusive nonintegrable system," Phys. Rev. Lett. **111**, 127205 (2013).

[6] Wen Wei Ho and Dmitry A. Abanin, "Entanglement dynamics in quantum many-body systems," Phys. Rev. B **95**, 094302 (2017).

[7] Jens H. Bardarson, Frank Pollmann, and Joel E. Moore, "Unbounded growth of entanglement in models of many-body localization," Phys. Rev. Lett. **109**, 017202 (2012).

[8] Y. Zhao, F. Andraschko, and J. Sirker, "Entanglement entropy of disordered quantum chains following a global quench," Phys. Rev. B **93**, 205146 (2016).

[9] Marko Žnidarič, Tomaž Prosen, and Peter Prelovšek, "Many-body localization in the Heisenberg XXZ magnet in a random field," Phys. Rev. B **77**, 064426 (2008).

[10] Maksym Serbyn, Z. Papić, and Dmitry A. Abanin, "Universal slow growth of entanglement in interacting strongly disordered systems," Phys. Rev. Lett. **110**, 260601 (2013).

[11] Didier Poilblanc, "Out-of-equilibrium correlated systems: Bipartite entanglement as a probe of thermalization," Phys. Rev. B **84**, 045120 (2011).

[12] Ming-Chiang Chung, Yi-Hao Jhu, Pochung Chen, and Chung-Yu Mou, "Quench dynamics of topological maximally entangled states," Journal of Physics: Condensed Matter **25**, 285601 (2013).

[13] Maurizio Fagotti and Fabian H. L. Essler, "Reduced density matrix after a quantum quench," Phys. Rev. B **87**, 245107 (2013).

[14] Elena Canovi, Elisa Ercolessi, Piero Naldesi, Luca Taddia, and Davide Vodola, "Dynamics of entanglement entropy and entanglement spectrum crossing a quantum phase transition," Phys. Rev. B **89**, 104303 (2014).

[15] Claudio Chamon, Alioscia Hamma, and Eduardo R. Mucciolo, "Emergent irreversibility and entanglement spectrum statistics," Phys. Rev. Lett. **112**, 240501 (2014).

[16] G Torlai, L Tagliacozzo, and G De Chiara, "Dynamics of the entanglement spectrum in spin chains," Journal of Statistical Mechanics: Theory and Experiment **2014**, P06001 (2014).

[17] Alejandro Zamora, Javier Rodríguez-Laguna, Maciej Lewenstein, and Luca Tagliacozzo, "Splitting a critical spin chain," Journal of Statistical Mechanics: Theory and Experiment **2014**, P09035 (2014).

[18] Abolfazl Bayat, Sougato Bose, Henrik Johannesson, and Pasquale Sodano, "Universal single-frequency oscillations in a quantum impurity system after a local quench," Phys. Rev. B **92**, 155141 (2015).

[19] Yi-Hao Jhu, Pochung Chen, and Ming-Chiang Chung, "Relaxation of the entanglement spectrum in quench dynamics of topological systems," Journal of Statistical Mechanics: Theory and Experiment **2017**, 073105 (2017).

[20] Zhi-Cheng Yang, Alioscia Hamma, Salvatore M. Giampaolo, Eduardo R. Mucciolo, and Claudio Chamon, "Entanglement complexity in quantum many-body dynamics, thermalization, and localization," Phys. Rev. B **96**, 020408 (2017).

[21] T. Rakovszky, S. Gopalakrishnan, S. A. Parameswaran, and F. Pollmann, "Signatures of information scrambling in the dynamics of the entanglement spectrum," Phys. Rev. B **100**, 125115 (2019).

[22] Zongping Gong, Naoto Kura, Masatoshi Sato, and Masahito Ueda, "Lieb-Robinson Bounds on Entanglement

Gaps from Symmetry-Protected Topology," arXiv e-prints , arXiv:1904.12464 (2019), arXiv:1904.12464 [quant-ph].
[23] Ronny Thomale, D. P. Arovas, and B. Andrei Bernevig, "Nonlocal order in gapless systems: Entanglement spectrum in spin chains," Phys. Rev. Lett. **105**, 116805 (2010).
[24] Rex Lundgren, Jonathan Blair, Martin Greiter, Andreas Läuchli, Gregory A. Fiete, and Ronny Thomale, "Momentum-space entanglement spectrum of bosons and fermions with interactions," Phys. Rev. Lett. **113**, 256404 (2014).
[25] G. Ehlers, J. Sólyom, Ö. Legeza, and R. M. Noack, "Entanglement structure of the hubbard model in momentum space," Phys. Rev. B **92**, 235116 (2015).
[26] Rex Lundgren, Jonathan Blair, Pontus Laurell, Nicolas Regnault, Gregory A. Fiete, Martin Greiter, and Ronny Thomale, "Universal entanglement spectra in critical spin chains," Phys. Rev. B **94**, 081112 (2016).
[27] Miguel Ibáñez-Berganza, Javier Rodríguez-Laguna, and Germán Sierra, "Fourier-space entanglement of spin chains," Journal of Statistical Mechanics: Theory and Experiment **2016**, 053112 (2016).
[28] Benedikt Herwerth, Germán Sierra, J. Ignacio Cirac, and Anne E. B. Nielsen, "Bosonic gaussian states from conformal field theory," Phys. Rev. B **98**, 115156 (2018).
[29] Balázs Dóra, Izabella Lovas, and Frank Pollmann, "Distilling momentum-space entanglement in luttinger liquids at finite temperature," Phys. Rev. B **96**, 085109 (2017).
[30] Timothy H. Hsieh and Liang Fu, "Bulk entanglement spectrum reveals quantum criticality within a topological state," Phys. Rev. Lett. **113**, 106801 (2014).
[31] Timothy H. Hsieh, Liang Fu, and Xiao-Liang Qi, "Tensor network implementation of bulk entanglement spectrum," Phys. Rev. B **90**, 085137 (2014).
[32] Qiong Zhu, Xin Wan, and Guang-Ming Zhang, "Topologically distinct critical theories emerging from the bulk entanglement spectrum of integer quantum hall states on a lattice," Phys. Rev. B **90**, 235134 (2014).
[33] Takahiro Fukui and Yasuhiro Hatsugai, "Entanglement chern number for an extensive partition of a topological ground state," Journal of the Physical Society of Japan **83**, 113705 (2014), https://doi.org/10.7566/JPSJ.83.113705.
[34] Ian Mondragon-Shem, Mayukh Khan, and Taylor L. Hughes, "Characterizing disordered fermion systems using the momentum-space entanglement spectrum," Phys. Rev. Lett. **110**, 046806 (2013).
[35] Ian Mondragon-Shem and Taylor L. Hughes, "Signatures of metal-insulator and topological phase transitions in the entanglement of one-dimensional disordered fermions," Phys. Rev. B **90**, 104204 (2014).
[36] Eric C Andrade, Mark Steudtner, and Matthias Vojta, "Anderson localization and momentum-space entanglement," Journal of Statistical Mechanics: Theory and Experiment **2014**, P07022 (2014).
[37] Longyan Gong, Ling Wei, Shengmei Zhao, and Weiwen Cheng, "Comparison of shannon information entropies in position and momentum space for an electron in one-dimensional nonuniform systems," Phys. Rev. E **86**, 061122 (2012).
[38] B.-T. Ye, Z.-Y. Han, L.-Z. Mu, and H. Fan, "Investigating disordered many-body system with entanglement in momentum space," Scientific Reports **7**, 16668 (2017).
[39] Vijay Balasubramanian, Michael B. McDermott, and Mark Van Raamsdonk, "Momentum-space entanglement and renormalization in quantum field theory," Phys. Rev. D **86**, 045014 (2012).
[40] Leopoldo A. Pando Zayas and Norma Quiroz, "Left-right entanglement entropy of boundary states," Journal of High Energy Physics **2015**, 110 (2015).
[41] Diptarka Das and Shouvik Datta, "Universal features of left-right entanglement entropy," Phys. Rev. Lett. **115**, 131602 (2015).
[42] Marika Taylor, "Generalized entanglement entropy," Journal of High Energy Physics **2016**, 40 (2016).
[43] Giandomenico Palumbo, "Momentum-space cigar geometry in topological phases," The European Physical Journal Plus **133**, 23 (2018).
[44] D. W. F. Alves and G. Camilo, "Momentum-space entanglement after smooth quenches," European Physical Journal C **79**, 48 (2019).
[45] Balázs Dóra, Rex Lundgren, Mark Selover, and Frank Pollmann, "Momentum-space entanglement and loschmidt echo in luttinger liquids after a quantum quench," Phys. Rev. Lett. **117**, 010603 (2016).
[46] T. Xiang, "Density-matrix renormalization-group method in momentum space," Phys. Rev. B **53**, R10445–R10448 (1996).
[47] Johannes Motruk, Michael P. Zaletel, Roger S. K. Mong, and Frank Pollmann, "Density matrix renormalization group on a cylinder in mixed real and momentum space," Phys. Rev. B **93**, 155139 (2016).
[48] David H. Dunlap, H-L. Wu, and Philip W. Phillips, "Absence of localization in a random-dimer model," Phys. Rev. Lett. **65**, 88–91 (1990).
[49] H.-L. Wu, William Goff, and Philip Phillips, "Insulator-metal transitions in random lattices containing symmetrical defects," Phys. Rev. B **45**, 1623–1628 (1992).
[50] Mohammad Pouranvari and Kun Yang, "Maximally entangled mode, metal-insulator transition, and violation of entanglement area law in noninteracting fermion ground states," Phys. Rev. B **89**, 115104 (2014).
[51] Mohammad Pouranvari and Afshin Montakhab, "Sensitivity of the entanglement spectrum to boundary conditions as a characterization of the phase transition from delocalization to localization," Phys. Rev. B **96**, 045123 (2017).
[52] Ingo Peschel, "Calculation of reduced density matrices from correlation functions," Journal of Physics A: Mathematical and General **36**, L205 (2003).
[53] The single-particle energy spectrum varies slightly for different disorder configurations. As such, when disorder averaging, we fix the number of total particles and only keep disorder configurations where E_F is within a small energy range about about the desired E_F ($E_F \pm .05$).
[54] Armin Rahmani and Smitha Vishveshwara, "Interplay of anderson localization and quench dynamics," Phys. Rev. B **97**, 245116 (2018).
[55] Yangang Chen and Guifre Vidal, "Entanglement contour," Journal of Statistical Mechanics: Theory and Experiment **2014**, P10011 (2014).
[56] N. Y. Yao, C. R. Laumann, J. I. Cirac, M. D. Lukin, and J. E. Moore, "Quasi-many-body localization in translation-invariant systems," Phys. Rev. Lett. **117**, 240601 (2016).
[57] Max McGinley, Andreas Nunnenkamp, and Johannes Knolle, "Slow growth of out-of-time-order correlators and entanglement entropy in integrable disordered systems," Phys. Rev. Lett. **122**, 020603 (2019).
[58] Daniel Hetterich, Maksym Serbyn, Fernando Domínguez, Frank Pollmann, and Björn Trauzettel, "Noninteracting central site model: Localization and logarithmic entanglement growth," Phys. Rev. B **96**, 104203 (2017).
[59] Yang Zhao and Jesko Sirker, "Logarithmic entanglement growth in two-dimensional disordered fermionic systems,"

Phys. Rev. B **100**, 014203 (2019).

[60] J. Schachenmayer, B. P. Lanyon, C. F. Roos, and A. J. Daley, "Entanglement growth in quench dynamics with variable range interactions," Phys. Rev. X **3**, 031015 (2013).

[61] Alessio Lerose and Silvia Pappalardi, "Origin of the slow growth of entanglement entropy in long-range interacting systems," arXiv e-prints , arXiv:1811.05505 (2018), arXiv:1811.05505 [cond-mat.stat-mech].

[62] Rajeev Singh, Roderich Moessner, and Dibyendu Roy, "Effect of long-range hopping and interactions on entanglement dynamics and many-body localization," Phys. Rev. B **95**, 094205 (2017).

[63] Ranjan Modak and Tanay Nag, "Many-body dynamics in long-range hopping model in the presence of correlated and uncorrelated disorder," arXiv e-prints , arXiv:1903.05099 (2019), arXiv:1903.05099 [cond-mat.dis-nn].

[64] For many-body localization, dephasing due to interactions is responsible for slow entanglement growth [10]. One can immediately rule out dephasing due to interactions being responsible for slow growth in our case as interactions are absent. However, dephasing due to some other mechanism can not be ruled out.

[65] R. Thomale, A. Sterdyniak, N. Regnault, and B. Andrei Bernevig, "Entanglement gap and a new principle of adiabatic continuity," Phys. Rev. Lett. **104**, 180502 (2010).

[66] Pablo Ordejón, Gerardo Ortiz, and Philip Phillips, "Localization in the interacting-random-dimer model," Phys. Rev. B **50**, 14682–14685 (1994).

[67] H. J. Changlani, N. M. Tubman, and T. L. Hughes, "Charge density waves in disordered media circumventing the Imry-Ma argument," Scientific Reports **6**, 31897 (2016).